

# $\gamma$ -Adaptin Appendage Domain: Structure and Binding Site for Eps15 and $\gamma$ -Synergin

Helen M. Kent,<sup>1</sup> Harvey T. McMahon,<sup>1</sup>

Philip R. Evans,<sup>1</sup> Alexandre Benmerah,<sup>2</sup>

and David J. Owen<sup>1,3,4</sup>

<sup>1</sup>MRC Laboratory of Molecular Biology

Hills Road

Cambridge CB2 2QH

United Kingdom

<sup>2</sup>INSERM Emi 0212

Faculté Necker-Enfants Malades

156, rue de Vaugirard

75730 Paris Cedex 15

France

## Summary

The AP1 complex is one of a family of heterotetrameric clathrin-adaptor complexes involved in vesicular trafficking between the Golgi and endosomes. The complex has two large subunits,  $\gamma$  and  $\beta$ , which can be divided into trunk, hinge, and appendage domains. The 1.8 Å resolution structure of the  $\gamma$  appendage is presented. The binding site for the known  $\gamma$  appendage ligand  $\gamma$ -synergin is mapped through creation of point mutations designed on the basis of the structure. We also show that Eps15, a protein believed to be involved in vesicle formation at the plasma membrane, is also a ligand of  $\gamma$  appendage and binds to the same site as  $\gamma$ -synergin. This observation explains the demonstrated brefeldinA (BFA)-sensitive colocalization of Eps15 and AP1 at the Golgi complex.

## Introduction

Transmembrane proteins and phospholipids are trafficked between intracellular compartments and the plasma membrane in carrier vesicles. Once the appropriate cargo has been sorted and concentrated into a forming vesicle, the vesicle buds from the donor membrane and is transported to, and then fuses with, the target membrane. One of the major classes of transport vesicles is the clathrin-coated vesicle (CCV) in which the phospholipid bilayer envelope is surrounded by a scaffold comprised of the protein clathrin. These two layers are linked by adaptor molecules that can crosslink clathrin directly with integral membrane protein cargo as in the case of the GGAs [1–4] or with phospholipid headgroups, e.g., AP180 and epsin [5, 6] or simultaneously with both as with the heterotetrameric AP complexes [7–10].

Four distinct AP complexes have been identified in higher eukaryotes (AP1, AP2, AP3, and AP4) and each is believed to be associated with a different trafficking pathway [11, 12]. AP1 is associated with the *trans*-Golgi

network (TGN) [13, 14] and endosomes [15] and is believed to mediate trafficking between TGN and the endosomal system, whereas AP2 is found in plasma membrane clathrin-coated pits (CCPs) and functions in clathrin-mediated endocytosis (CME) [14, 16]. All AP complexes are heterotetramers comprised of two large (100–130 kDa) adaptin subunits, which can be subdivided into a trunk domain (65–70 kDa) and an appendage or ear domain (15–35 kDa) linked by an extended flexible linker or hinge (see Figure 1D), a medium adaptin subunit of approximately 50 kDa, and a small adaptin subunit of 15–17 kDa (reviewed in [11]). Various functions have been ascribed to different domains of AP complex subunits. The Yxx $\phi$  tyrosine-based sorting signals bind to the medium ( $\mu$  subunit) [9, 17] while the D/E $xx$ LL dileucine-based motifs may bind to the trunks of the  $\beta$  subunits [18] and/or the medium chains [19]. In the case of AP2, the  $\alpha$  trunk binds to phospholipid headgroups [6, 10]. Clathrin interacts, via its terminal domain, with L $\phi$ n $\phi$ D/E clathrin box motifs in the hinge regions of  $\beta$ - and  $\gamma$ -adaptins [8, 20–22]. The appendage domains of AP2 $\alpha$  and  $\beta$  subunits recruit a number of proteins that perform accessory/regulatory roles in CCV biogenesis: these include Eps15, epsin, AP180, auxilin, and the amphiphysins [23–27]. The three-dimensional structures of the  $\alpha$  and  $\beta$  appendage domains have been solved and have lead to an understanding of how they interact with their binding partners [25, 26, 28]. Less is known of the exact roles of the large subunit appendage domains of the AP1 adaptor complex. Several candidate binding partners have been identified for the  $\gamma$  appendage, which include the EH domain-containing protein  $\gamma$ -synergin [29]. The appendage domain of  $\gamma$  is approximately half the size (120 amino acids) of the other appendage domains (250–300 amino acids) (see Figure 1). Domains of similar sequence have been recently identified in another set of proteins termed the GGAs (Golgi localized gamma ear containing ARF1 binding proteins), which are involved in vesicle coat formation and have been implicated in trafficking between the TGN and endosomes [30–32].

Here we present the structure of a part of the AP1 adaptor complex—the  $\gamma$ -adaptin appendage domain determined by X-ray crystallography at 1.8 Å resolution. It is an eight-stranded  $\beta$  sandwich similar to the N-terminal subdomain of the  $\alpha$  appendage [25] with which it has 12% sequence identity on the basis of a structural alignment (see Figure 1D). In the  $\alpha$  appendage this domain has no function assigned to it other than correctly presenting the C-terminal, protein binding “platform” subdomain [28], and yet in the  $\gamma$  appendage it performs the protein recruitment role. Structure-directed mutagenesis was used to locate the binding site for the EH domain-containing protein  $\gamma$ -synergin to a shallow hydrophobic trough formed where the two  $\beta$  sheets meet. A second EH domain-containing protein Eps15, pre-

<sup>3</sup>Correspondence: djo30@cam.ac.uk

<sup>4</sup>Present address: Cambridge Institute for Medical Research, Department of Clinical Biochemistry, Wellcome Trust/MRC Building, Hills Road, Cambridge CB2 2XY, United Kingdom.

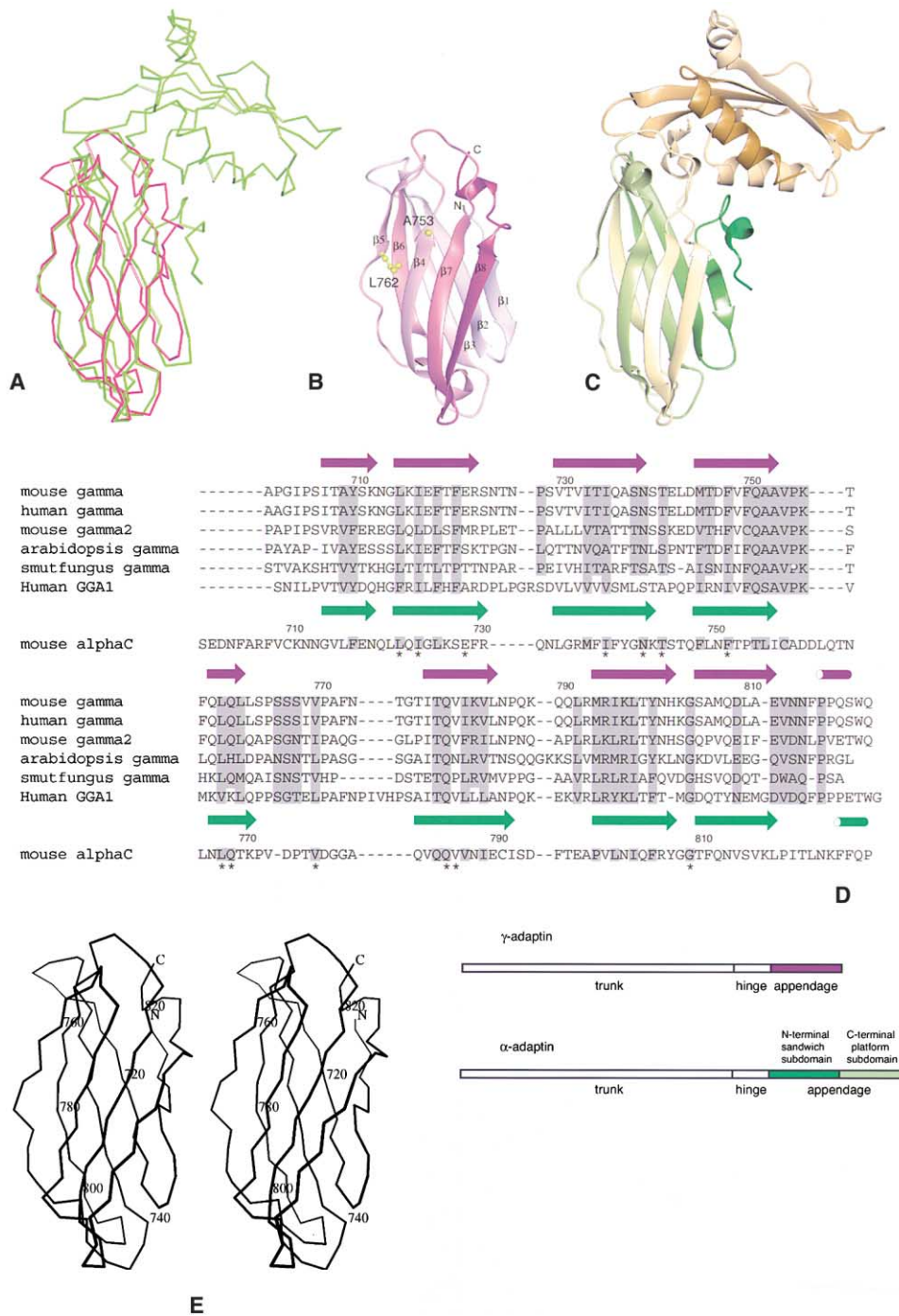


Figure 1. Comparison of the Structures of the  $\gamma$  and  $\alpha$  Appendages

(A) Superposition of the  $C_{\alpha}$  traces of  $\gamma$  appendage (purple) and  $\alpha$  appendage N-terminal subdomain (green). The two overlap with an rms deviation of 1.8 Å for 96  $C_{\alpha}$  atoms.

(B) Schematic representation of the  $\gamma$  appendage domain. Point mutations that abrogate binding to  $\gamma$ -synergic and Eps15 are shown in yellow in ball and stick representation. All protein structure pictures were made using Aesop (M.E.M. Noble, personal communication).

(C) Schematic representation of the  $\alpha$  appendage domain. The N-terminal subdomain is in green and the C-terminal subdomain in gold.

(D) Structure-based sequence alignment of  $\gamma$  appendages from human, mouse, *Arabidopsis*, and smutfungus, mouse  $\gamma$ 2-appendage, human GGA1 appendage, and the N-terminal subdomain of the  $\alpha$  appendage. The positions of  $\beta$  strands are marked by arrows and  $\alpha$  helices with rods (purple human  $\gamma$  appendage and green  $\alpha$  appendage). Conserved residues are indicated by gray shading and residues identical between the  $\gamma$  and  $\alpha$  appendages are marked with an asterisk.

(E)  $C_{\alpha}$  trace of the  $\gamma$  appendage in stereo representation.

viously shown to be a major binding partner of the  $\alpha$  appendage, is shown to bind to the same site on the  $\gamma$  appendage as  $\gamma$ -synergin. The interaction of  $\gamma$  appendage with Eps15 explains the BFA-sensitive colocalization of Eps15 and AP1 at the Golgi network, which we demonstrate by immunofluorescence.

## Results

### Structure of the $\gamma$ -Adaptin Appendage Domain

Sequence alignment programs failed to produce a statistically significant alignment of the  $\gamma$  appendage domain with the entire sequences of  $\alpha$  and  $\beta 2$  appendage domains and secondary structure prediction gave no obvious indication that the  $\gamma$  appendage was structurally similar to either the amino or carboxy terminal subdomains of  $\alpha$  or  $\beta 2$  appendage domains. The structure of the appendage domain of  $\gamma$ -adaptin (residues 704–822) was therefore determined by X-ray crystallography by isomorphous replacement at 1.8 Å resolution. The wild-type protein crystallized in space group P212121 with one molecule in the asymmetric unit. A single site xenon derivative, a weak PtCl<sub>4</sub><sup>2-</sup> derivative, and solvent flattening gave an excellent electron density map.

The structure of the  $\gamma$ -adaptin appendage domain is an eight-stranded  $\beta$  sandwich (Figures 1A and 1E) comprised of one eight-stranded and one five-stranded  $\beta$  sheet very similar to that of the amino-terminal subdomain of  $\alpha$ -adaptin (rms of 1.8 Å over 96 C $\alpha$ ; Figure 1A). The sheets are closer together at the edge where strands 1 and 8 meet than at the edge where strands 4 and 5 meet. On the basis of a superposition with the  $\alpha$  and  $\beta 2$  appendage domains, the structure-based sequence alignment shown in Figure 1D was constructed. There are 13 residues conserved between the  $\gamma$  appendage and the  $\alpha$  appendage amino-terminal subdomain. Ten of these are involved in maintaining the architecture of the fold. Of these, seven are amino acids with hydrophobic side chains, which pack the core of the sandwich, while the other three are vital in maintaining the backbone conformation of turns between strands. Comparison of the available  $\gamma$  appendage domain sequences from human, rodent, *Arabidopsis*, and fungus shows conservation of residues mainly within the  $\beta$  strands. The notable exception is the sequence QAAVPK in the loop between strands 4 and 5, which is identical in all the  $\gamma$  appendage sequences as well as in that of the GGA appendages (Figure 1D).

### Function of $\gamma$ Appendage Domain

Comparison of the  $\gamma$  and  $\alpha$  appendage structures shows that the  $\gamma$  appendage lacks the platform subdomain present in the  $\alpha$  appendage. This platform subdomain contains the single site through which the  $\alpha$  appendage binds to all of its known ligands. The N-terminal sandwich subdomain of the  $\alpha$ - and  $\beta 2$ -adaptins have no function assigned to them other than correctly presenting the platform protein/protein interaction subdomain. Since the  $\gamma$  appendage domain functions as a protein recruitment module [29], it was surprising that it resembled the N-terminal  $\beta$  sandwich subdomain rather than C-terminal protein binding platform subdomain of the

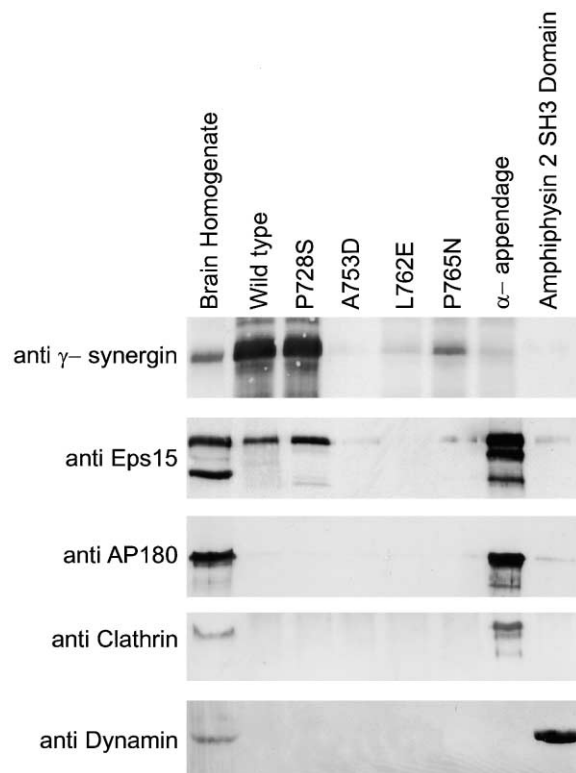


Figure 2. Interaction of  $\gamma$  Appendage with  $\gamma$ -Synergin and Eps15  
Purified, folded GST-fusion proteins corresponding to wild-type and mutant forms of  $\gamma$  appendage,  $\alpha$  appendage, and amphiphysin2 SH3 domain were used in pull-down experiments from rat brain cytosol (see Experimental Procedures). Wild-type and P728S (a control mutation distant from the binding site) bound to  $\gamma$ -synergin and Eps15, whereas P765N showed reduced binding, and L762E and A753D showed no binding. No form of the  $\gamma$  appendage bound significantly to AP180, dynamin, or clathrin.

$\alpha$  appendage. The appendage domains of  $\alpha$  and  $\gamma$  as N-terminal GST fusion proteins were used in pull-down experiments, the results of which were probed with antibodies specific to known ligands of the various appendage domains (Figure 2; Table 2). The  $\alpha$  appendage domain was confirmed to interact with Eps15, AP180, and also weakly with clathrin (Figure 2) but not with dynamin (Figure 2 and [25, 28]) or the 110 kDa  $\gamma$ -synergin (Figure 2). The  $\gamma$  appendage domain binds to  $\gamma$ -synergin as expected [29] but not significantly to clathrin (which has been proposed to be a direct ligand for the  $\gamma$  hinge [22]), AP180, the amphiphysins, or dynamin. However, it was able to bind to the largest of the four Eps15 isoforms present in brain, all of which bind to the  $\alpha$  appendage.

The  $\gamma$  appendage binds its partners with high micromolar dissociation constant (as estimated from the low stoichiometry of ligand to appendage present in GST pull-down experiments when assayed by Coomassie blue staining; data not shown). This is a similar affinity to that of the  $\alpha$  and  $\beta 2$  appendages for their binding partners [25, 26], so a similar binding mode through the recognition of a short peptide motif would be expected. The surface was therefore inspected for suitable sites that could accommodate a short peptide motif and

Table 1. Binding of Ligands to Wild-Type and Mutant  $\gamma$  Appendages

	$\gamma$ -Synergin	Eps15	Clathrin	AP180	Dynamin1
$\gamma$ appendage	+++	++			
P728S	+++	++			
A753D					
L762E					
P765N	+	+			
$\alpha$ appendage	-/+	+++	+	+++	
Amph2 SH3					+++

Summary of data from pull-down experiments using GST-fusion proteins of wild-type and mutant forms of the  $\gamma$  appendage,  $\alpha$  appendage, and the amphiphysin2 SH3 domain. The degree of binding is indicated by the number of + symbols (no binding above background is indicated by -). The results shown are the average of eight independent experiments. P728 is distant from the binding site, and the mutant P728S is included as a control. Other mutations which show wild-type binding behavior are: N713W, R723E, V749N, Q751S, V754T, K756E, Q759H, L760Q, L763E, S764A, S768A, Y800F, H802S, L810P, and W821G. Mutation in Q780 to A, K, or N cause unfolding.

had at least moderate hydrophobic surface potential [25]. Unlike the situation with the  $\alpha$  and  $\beta$  appendages, no obvious site of high-hydrophobic potential was revealed.

A variety of point mutations were made on the basis of the structure, mainly in surface residues that did not appear to be involved in maintaining the integrity of the protein fold (see complete list in the legend to Table 1, illustrated in Figure 3A). The mutants were made as N-terminal GST fusion proteins, the GST proteolytically cleaved, and the fold of each resulting  $\gamma$  appendage domain was tested by circular dichroism (data not shown). All were folded except mutations in Q780, which resulted in insoluble protein. This residue is conserved between  $\alpha$  and  $\gamma$  appendages, and the effect of mutating it may be explained by the partial burial of the hydrophilic side chain of this residue (Figure 3A). The folded

N-terminal GST fusion proteins were used in pull-down experiments from brain cytosol; the results of which were probed with antibodies against  $\gamma$ -synergin and AP2 ligands as described above (Figure 2; and summarized in Table 1). Two point mutations were identified that prevented binding of  $\gamma$ -synergin and Eps15 (A753D and L762E) and one that reduced their binding (P765N).

These mutations map to a shallow trough lined with mainly hydrophobic residues on the surface formed where  $\beta$  strand 4 from the three-stranded sheet and strand 5 from the five-stranded sheet meet (as shown in Figures 3A and 3B). In the center of this trough there is a small hydrophobic pocket lined by the side chains of L762, L760, and I782. The effects of the mutations at the molecular level were probed by crystallizing the mutant forms of the protein. The mutant L762E crystallized in the same crystal form as the native  $\gamma$  appendage

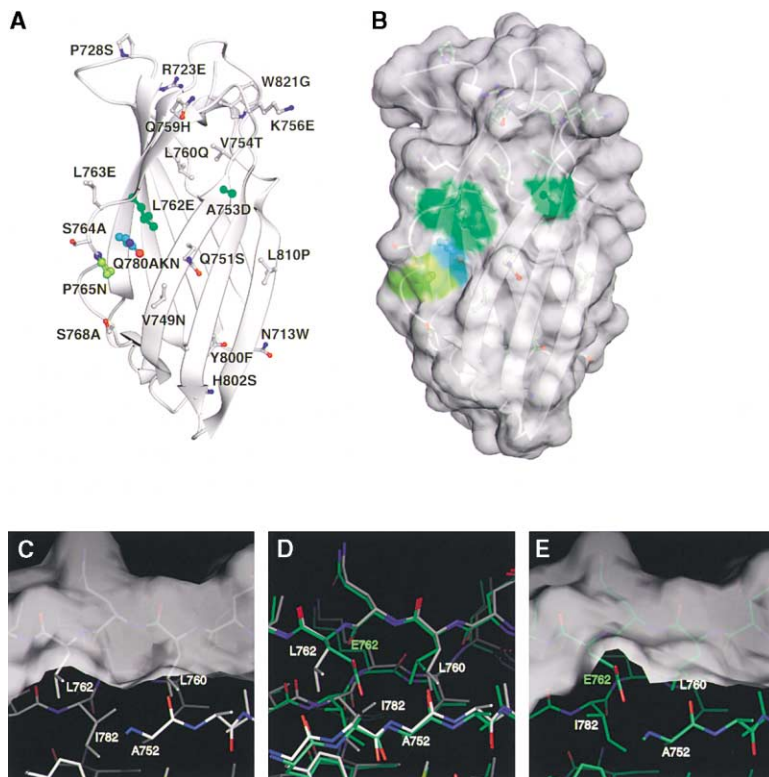
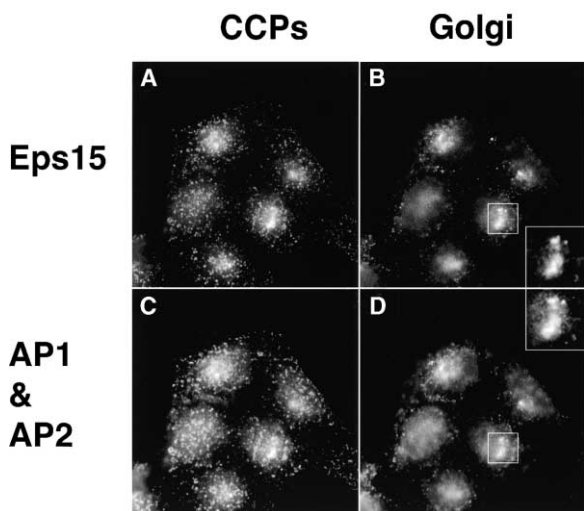


Figure 3. Mutations L762E and A753D Abolish Ligand Binding but Do Not Effect the Fold of  $\gamma$  Appendage

(A) Schematic representation of  $\gamma$  appendage with all the side chains that were mutated shown in ball and stick representation. Mutations that cause altered binding of  $\gamma$ -synergin and Eps15 are colored bright green (abolition of binding), pale green (partial binding), and no effect (uncolored). Q780, which unfolds the protein, is colored blue.

(B) Surface representation of  $\gamma$  appendage calculated using Aesop (M.E.M. Noble, personal communication) to show the hydrophobic trough between strands 4 and 5. Mutations are colored according to the effect of the mutation on  $\gamma$ -synergin/Eps15 binding as in (A).

(C-E) The L762E mutation causes the small hydrophobic pocket formed by L760, L762, and I782 to become blocked. The wild-type  $\gamma$  appendage structure is shown with carbon atoms in white (C and D) and the L762E mutant structure with carbon atoms in green (D and E). (D) is a superposition of wild-type and L762E. (C)-(E) are taken from the same viewpoint.



**Figure 4. Eps15 Is Present on the Plasma Membrane and the Golgi**  
HeLa cells were fixed, permeabilized, and processed for immunofluorescence microscopy using a rabbit affinity-purified anti-Eps15 polyclonal antibody (A and B) and the anti- $\beta$ -adaptins monoclonal mouse antibody 100.1 (C and D), revealed by Alexa 594-labeled anti-rabbit immunoglobulins and Alexa 488-labeled anti-mouse immunoglobulins secondary antibodies. Cells were observed under an epifluorescence microscope attached to a cooled CCD camera. In (A) and (C), the focus was made on the planar plasma membrane adherent to the coverslip to better observe CCPs. In (B) and (D), the focus was made on the central region of the cell to better observe the Golgi apparatus. The same field is shown (A)–(D). In (B) and (D), insets show a higher magnification ( $\times 2$ ) of the portions of cells included in the open squares.

domain, whereas the A753D crystallized in the space group P41212 with two rather than one molecule in the asymmetric unit. There are no significant movements in the peptide backbones of either mutant directly caused by the mutations.

In the case of the L762E mutation, the glutamate side chain moves to allow its carboxyl group to point into solvent and results in the pocket created by L762, L760, and I782 becoming filled (Figure 3). The side chain of residue L760 has moved more into the core of the protein in order to try and compensate for the loss of the L762 side chain from this region. The A753D mutant shows no significant changes in the side chains that make up the small hydrophobic pocket (data not shown).

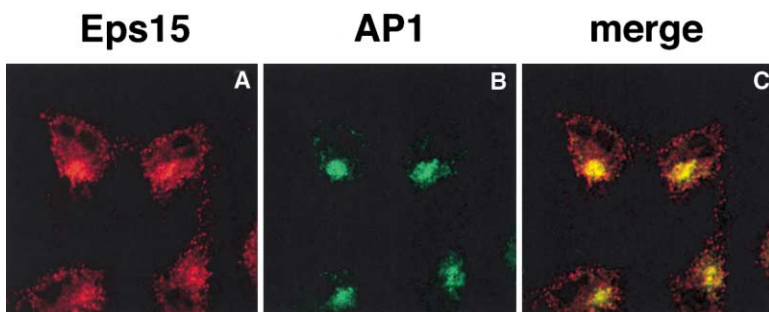


**Figure 5. Colocalization of Eps15 and AP1 at the Golgi**

HeLa cells were fixed, permeabilized, and processed for immunofluorescence microscopy using the affinity-purified anti-Eps15 antibody (A) and the anti- $\gamma$ -adaptin mouse monoclonal antibody 100.3 (B), revealed by an Alexa 594-labeled anti-rabbit immunoglobulins and an Alexa 488-labeled anti-mouse immunoglobulins secondary antibodies. Cells were observed under a confocal microscope. A medial optical cut of representative cells is shown. Areas of colocalization appear yellow in the computer-generated composite image (C).

### Role of AP1 In Vivo

Is the interaction of the  $\gamma$  appendage with Eps15, which has been demonstrated in vitro (see above), relevant in vivo? It has been previously reported that, in addition to its colocalization with AP2 at the plasma membrane, Eps15 shows some perinuclear staining that is sensitive to nocodazole treatment [33, 34]. These results suggested a possible dual localization of Eps15 to plasma membrane CCPs and clathrin-coated regions of the Golgi, i.e., the TGN. To test this hypothesis, HeLa cells were fixed and stained for Eps15 (Figures 4A and 4B) and both AP1 and AP2 (Figures 4C and 4D) using an antibody against  $\beta$ 1- and  $\beta$ 2-adaptins. Eps15 showed a complete colocalization with punctate plasma membrane-associated AP2 (CCPs) and significant colocalization with perinuclear Golgi AP1 staining (TGN) (see insets Figure 4). The Eps15/AP1 colocalization is further demonstrated by the amount of yellow coloration at the Golgi in the merged image (Figure 5C) of Eps15 (Figure 5A, red) and AP1 (Figure 5B, green) obtained by confocal microscopy. The additional peripheral red punctate staining for Eps15 is due to the presence of Eps15 in CCPs at the plasma membrane. The same staining and colocalization pattern was observed using GFP-tagged Eps15 constructs (data not shown) confirming that TGN staining of Eps15 was not due to cross-reactivity of the antibodies with a related EH-domain-containing protein.

AP1 is recruited to membranes through its interaction with the small GTPase ARF1 only when ARF1 is in its membrane-associated GTP-bound form. The exchange of GDP for GTP on ARF1 is catalyzed by a guanine nucleotide exchange factor (GEF). BFA causes dissociation of AP1 from membranes through its ability to interfere with the GEF catalyzed GDP/GTP nucleotide exchange on ARF1 [35]. If proteins such as  $\gamma$ -synergin and Eps15 that do not bind to ARF1 show BFA-sensitive membrane localization, it must be because they interact with an ARF1 binding adaptor protein/protein complex such as AP1. The effect of BFA treatment on the localization of Eps15 was therefore investigated (Figure 6). Cells were treated with ethanol (Figures 6A–6C) or BFA (Figures 6C–6E), and the staining for Eps15 (Figures 6A, 6B, 6D, and 6E) and AP1 (Figures 6C and 6F) was studied using confocal microscopy focusing on the Golgi (Figures 6B, 6C, 6E, and 6F) or the plasma membrane (Figures 6A and 6D). Eps15 Golgi staining is lost in the same way as staining for AP1 (Figures 6B, 6C, 6E, and 6F), which is consistent with the localization of Eps15 being

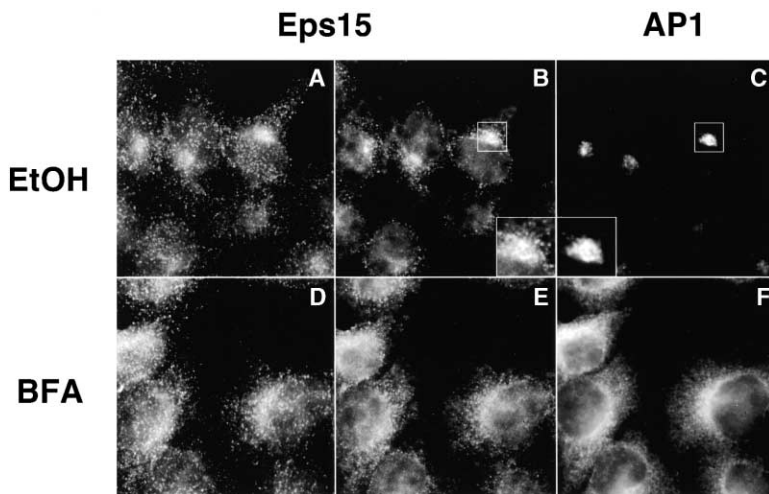


Figure 6. Eps15 Localization at the Golgi is BrefeldinA Sensitive

Ethanol- (A–C) and BFA- (D–F) treated HeLa cells were fixed and processed for immunofluorescence microscopy using the polyclonal affinity-purified anti-Eps15 antibody (A and B, and D and E) and the anti- $\gamma$ -adaptin monoclonal mouse antibody 100.3, revealed by an Alexa 488-labeled anti-rabbit immunoglobulins and an Alexa 594-labeled anti-mouse immunoglobulins secondary antibodies. Cells were observed under an epifluorescence microscope attached to a CCD camera. The same field is shown in (A)–(C), and in (D)–(F). In (A) and (D), the focus was made on the planar plasma membrane adherent to the coverslip to better observe CCPs. In (B)–(F), the focus was made on the central region of the cell to better observe the Golgi apparatus. In (B) and (C), insets show a higher magnification ( $\times 2$ ) of the portions of cells included in squares.

due to its interaction with AP1. A similar scenario for the BFA sensitivity of  $\gamma$ -synergin staining has been demonstrated [29]. In contrast to the Golgi staining of Eps15, plasma membrane CCP staining of Eps15 is not perturbed by BFA treatment (Figures 6A and 6D), as previously reported for AP2, since AP2 recruitment is not BFA sensitive [35].

## Discussion

The structure of the  $\gamma$ -adaptin appendage domain is very similar to that of the  $\alpha$ -adaptin N-terminal subdomain despite only 12% sequence identity: this similarity was detectable only after structure determination. Most of

the residues conserved between the  $\alpha$ - and  $\gamma$ -adaptin appendages are involved in maintaining the architecture of the fold either by packing the hydrophobic interior of the protein or maintaining structure in turns. This  $\beta$  sandwich domain is shown to have a protein binding function in the  $\gamma$  appendage, mediated by a shallow hydrophobic groove formed where the two sheets meet. The requirement that interactions between appendage domains and their ligands be transient, with  $K_d$ s in the high micromolar range, means that they are likely to involve a short peptide binding to a folded domain. The nature of the binding site, namely a shallow hydrophobic trough surrounded by charged (mainly basic) residues, is in line with this mode of interaction. This type of site is also found in the  $\alpha$  and  $\beta 2$  appendage domains, which bind to D $\phi$ F motifs [25, 26, 28], and in EH domains, which bind to NPF motifs [36]. All of the mutations (L762E, P765N, and A753D) alter the chemical properties of this potential binding site, in all cases making it less hydrophobic, which argues that a substantial part of the interaction will be mediated by hydrophobic side chain interactions. The L762E mutation also results in the filling in of the small hydrophobic cavity between L762 and L760, which would be a good candidate for the interaction site for a hydrophobic side chain. This small pocket does not have a high hydrophobic potential, as do the D $\phi$ F binding pockets in the  $\alpha$  and  $\beta 2$  appendages [25, 26], due to the presence of the backbone amide of residues A752 and K756 and the backbone carbonyl of residue A752. These backbone groups may well interact with the backbone of the motif on  $\gamma$ -synergin/Eps15 to which the  $\gamma$  appendage binds. It is also interesting to note that the mutations that have the largest effects on ligand binding both increase the local negative charge around the binding site on the  $\gamma$  appendage, suggesting that the interaction may also involve recognition of a negative charge on the target proteins. The N-terminal  $\beta$  sandwich domains in the  $\alpha$  and  $\beta 2$  appendages have different surface characteristics from the  $\gamma$  appendage  $\beta$  sandwich domain, which argues that in these larger appendages this domain does not play a protein/protein interaction role.

Did the  $\gamma$  appendage lose its platform domain or did

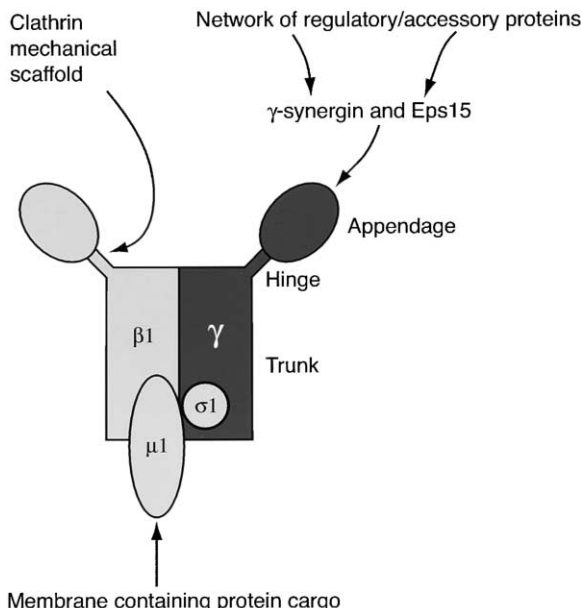


Figure 7. Role of  $\gamma$  Appendage in AP1 Function

The  $\gamma$  appendage recruits proteins including  $\gamma$ -synergin and Eps15, which may in turn recruit further proteins to aid in the formation of AP1-containing CCVs.

Table 2. Statistics on Data Collection and Phasing

Data collection <sup>a</sup>	Native	L762E
Resolution (Å) (outer bin)	1.81 (1.91)	1.70 (1.80)
$R_{\text{merge}}^b$	0.062 (0.242)	0.062 (0.279)
$R_{\text{meas}}^c$	0.073 (0.285)	0.067 (0.305)
$\langle\langle I \rangle\rangle/\sigma(\langle\langle I \rangle\rangle)$	15.1 (5.1)	22.0 (6.0)
Completeness (%)	98.7 (92.2)	99.6 (97.9)
Multiplicity	3.7 (3.6)	6.4 (6.1)
Wilson plot B (Å <sup>2</sup> )	20	20
MIR phasing	Xe	PtCl <sub>4</sub> <sup>2-</sup>
Number of sites	2	2
$R_{\text{cullis}}^d$	0.60	0.90
Phasing power: isomorphous (anomalous) <sup>e</sup>	2.2 (1.1)	0.94 (0.76)
Mean figure of merit	0.36	
Figure of merit after solvent flattening (all data)	0.92	
Refinement	Wild-type	L762E
$R (R_{\text{free}})^f$	0.175 (0.223)	0.178 (0.225)
$\langle B \rangle (\text{Å}^2)$	23.5	21.2
$N_{\text{reflections}} (N_{\text{free}})$	10724 (1164)	12740 (1408)
$N_{\text{atoms}} (N_{\text{water}})$	1114 (171)	1135 (191)
Rmsd bondlength (Å)	0.032	0.021
Rmsd angle (°)	2.2°	1.9°
Estimated coordinate error from $R_{\text{free}}$ (Å)	0.135	0.118
Number of Ramachandran violations	0	0

<sup>a</sup>Values in brackets apply to the high-resolution shell.

<sup>b</sup> $R_{\text{merge}} = \sum \sum_{ij} |I_{ij} - \bar{I}_h| / \sum \sum |I_{ij}|$ , where  $\bar{I}_h$  is the mean intensity for reflection  $h$ .

<sup>c</sup> $R_{\text{meas}} = \sum \sqrt{(n/(n-1)} |I_{ij} - \bar{I}_h| / \sum |I_{ij}|$ , the multiplicity weighted  $R_{\text{merge}}$  (Diederichs and Karplus, 1997).

<sup>d</sup> $R_{\text{cullis}} = \sum ||\mathbf{F}_{\text{PH}} - \mathbf{F}_p|| - ||\mathbf{F}_{\text{Hcalc}}|| / \sum ||\mathbf{F}_{\text{PH}} - \mathbf{F}_p||$ .

<sup>e</sup>Phasing power =  $\langle\langle |\mathbf{F}_{\text{Hcalc}}| \rangle\rangle / \text{phase-integrated lack of closure}$ .

<sup>f</sup> $R = \sum |\mathbf{F}_p - \mathbf{F}_{\text{calc}}| / \sum |\mathbf{F}_p|$ .

other appendage domains acquire it? Structure determination (adaptin appendages from  $\alpha$ ,  $\beta 2$ , [25, 26, 28], and  $\delta$  [unpublished data]) and sequence alignments ( $\beta 1$ ,  $\beta 3$ , and  $\epsilon$  adaptin appendages, and  $\beta$ COP and  $\gamma$ COP putative appendages) show the presence of large (30–35 kDa) two-subdomain appendages on these “large adaptin subunits.” Since  $\gamma$ - and  $\alpha$ -adaptins are the most closely related of these large adaptin proteins (on the basis of sequence alignments of their trunk domains), that is they diverged from each other after the divergence of the other large subunits [37], it seems probable that the  $\gamma$ -adaptin once had a two-subdomain appendage but lost its platform subdomain. The high degree of sequence identity between the  $\gamma$  and GGA appendages (Figure 1D) [30–32] clearly points to these domains having evolved from a common single domain ancestor more recently than the separation of  $\gamma$ -adaptin from  $\alpha$ -adaptin. The proposal that the appendage domains of  $\gamma$ -adaptin,  $\gamma 2$ -adaptin, and the GGAs perform the same functions, namely binding to the same protein ligands, is supported by the very high degree of sequence identity between them in the binding site (QAAVPKxxxSQL) identified in this work (Figure 1D).

The ability of  $\gamma$ -synergin and the largest isoform of Eps15 to bind to the  $\gamma$  appendage along with the colocalization of AP1 and Eps15 (this work) and of AP1 and  $\gamma$ -synergin [29], demonstrated by immunofluorescence microscopy, suggests that these pairs of proteins interact in vivo. This is supported by the observation that the Golgi localization of both these EH domain-containing proteins is disrupted by BFA, a compound that interferes

with the localization of proteins whose membrane binding is regulated by the small GTPase ARF1. AP1 has been shown to bind to ARF1 [38], but neither  $\gamma$ -synergin nor Eps15 bind to ARF1. The exact role played by either  $\gamma$ -synergin or Eps15 is unclear but is most likely to be in using their EH domains to recruit NPF-containing proteins, including epsin and synaptojanin (reviewed in [39]), needed for AP1-containing vesicle formation. A similar role has been proposed for Eps15 function in CME at the plasma membrane. Obvious candidates for recruitment by Eps15/ $\gamma$ -synergin at the Golgi would be members of the epsin family, which may explain the observation that there is a pool of epsin located at the Golgi [24]. The  $\gamma$  appendage functions as a site for recruitment of proteins that play accessory/regulatory roles in AP1-containing CCV formation, which include  $\gamma$ -synergin and Eps15 and, in all probability, further proteins that remain to be identified.

### Biological Implications

The structure of the AP1  $\gamma$  appendage has a  $\beta$  sandwich fold. It is therefore structurally similar to the N-terminal subdomains of the AP2  $\alpha$  and  $\beta 2$  appendages, although it performs the same function as the C-terminal subdomains of these larger appendages, namely recruitment of proteins that play accessory roles in CCV formation. The binding site on the  $\gamma$  appendage for the established ligand  $\gamma$ -synergin is situated where the two sheets of the sandwich meet and is shown to be the same site where the newly proposed ligand, Eps15, also binds.

Eps15 resembles  $\gamma$ -synergin in its BFA-sensitive colocalization with AP1 at the Golgi, suggesting that Eps15 functions at the Golgi as well as at the plasma membrane where it is involved in CME. This indicates a general role for Eps15 in CCV formation and therefore raises questions about the use of Eps15 domains as specific inhibitors of CME. Some of the proteins that interact directly with the AP2 complex appendages, such as Eps15 and amphiphysin, also bind to other proteins, such as epsin, dynamin, and synaptosomal protein. The finding that both the ligands of the  $\gamma$  appendage contain protein/protein interaction "EH" domains suggests that a similarly large network of proteins may be recruited during both AP1- and AP2-containing CCV formation (Figure 7).

The identification of single point mutations that prevent  $\gamma$ -synergin binding will be useful tools for investigating the function AP1 in vivo. The transfer of the L762E and/or A753D mutations to full-length  $\gamma$ -adaptin so that it is unable to interact with  $\gamma$ -synergin and Eps15 will make it possible to investigate the role of these interactions in AP1 function. The mutations described may knock out the AP1 pathway, thus making it possible to demonstrate exactly which pathway(s) use AP1 as an adaptor. Further, it should also allow the role of  $\gamma$ -synergin and Eps15 to be investigated.

#### Experimental Procedures

##### Constructs

The cDNA encoding residues 704–822 of mouse  $\gamma$ -adaptin (the appendage domain) was cloned into the vector pGEX 4T2 for production as an N-terminal GST fusion protein and into pET15b for expression as an N-terminal hexahis-tagged fusion. Mutants of  $\gamma$  appendage were made by PCR using primers incorporating the changed bases.

##### Protein Expression and Purification

GST-fusion protein for biochemical studies were expressed in DH5 $\alpha$  at 25°C overnight and produced as in [25]. N-terminal His<sub>6</sub>-tagged fusion proteins for crystallization trials were grown in bacterial strain BL21DE3 pLysS at 25°C overnight. The proteins were purified on a Ni-NTA-agarose column (Qiagen) and bound protein was eluted with buffer A (0.2 M NaCl, 20 mM HEPES [pH 7], 4 mM  $\beta$ -mercaptoethanol) containing 0.3 M imidazole. The proteins were further purified on S200 gel filtration and subsequently dialyzed into 5 mM HEPES, 50 mM NaCl, and 4 mM DTT, and concentrated to 5 mg/ml.

##### Crystallization and Structure Determination of $\gamma$ Appendage Domain

Crystals of wild-type and L762E were grown by hanging drop vapor diffusion against a reservoir containing 50 mM HEPES [pH 7.4], 0.9 M Na<sup>+</sup>/K<sup>+</sup> Tartrate, 20% w/v glycerol. Crystals were of space group P212121 with one molecule in the asymmetric unit, unit cell dimensions a = 34.1 Å, b = 54.8 Å, and c = 68.0 Å. The mutant A753D crystallized in the spacegroup P41212 with two molecules in the asymmetric unit, unit cell dimensions a = b = 62.2 Å and c = 148.9 Å, grown by hanging drop vapor diffusion against a reservoir containing 24% PEG4000, 100 mM Tris (pH 8.0), and 200 mM MgCl<sub>2</sub>.

X-ray diffraction data were collected at 100 K in-house on a rotating anode (Table 2). A xenon derivative was made by placing a crystal in a sealed chamber into which xenon was forced to 12 atmospheres pressure for 10 min. The Pt derivative was made by soaking the crystal in buffer containing 1 mM PtCl<sub>4</sub><sup>2-</sup> for 2 hr. Data were recorded on a MAR345 detector, integrated with MOSFLM [40], and scaled using Scala [41]. The xenon site was determined from difference Pattersons, and heavy-atom refinement and phasing were performed with SHARP [42], followed by solvent flipping and flattening with SOLOMON [43], leading to an excellent electron density map at 1.8 Å resolution. The model was built with O [44] and

refined with REFMAC [45]. Hydrophobic interaction surface potentials were calculated as in [25] and displayed using Aesop (M.E.M. Noble, personal communication).

##### Protein-Protein Binding Assays

Binding assays were performed by incubating 20 µg GST $\gamma$  appendage or GST amphiphysin2 SH3 domain or 30 µg GST $\alpha$  appendage with 0.5 ml of 0.1% TritonX-100 brain extract in buffer A in the presence of 20 µl 50% slurry of glutathione-sepharose at 4°C for 1 hr. The beads were washed three times for 3 min with buffer A and the bound proteins analyzed by SDS PAGE followed by immunoblotting. One fifth of each pull-down experiment was loaded on each lane, i.e., 4 µg GST $\gamma$  appendage. Antibodies used were: anti-AP180 (NB29 Oncogene), anti-eps15 (C-20 Santa Cruz Laboratories), and anti-clathrin heavy chain (TD1 Neomarkers), anti-dynamin (NB28 Oncogene), and anti- $\gamma$ -synergin (HMK1).

##### Immunofluorescence

HeLa cells (ATCC, Manassas, VA) were grown in Eagle's medium modified by Dulbecco (DMEM), supplemented with 10% fetal calf serum, 2 mM L-glutamine, penicillin, and streptomycin (GIBCO-BRL). For treatment with BFA (Sigma), HeLa cells grown on coverslips were incubated for 2 min at 37°C with 5 µg/ml BFA in DMEM or with a 1/2000 dilution of ethanol in DMEM as a control.

For immunofluorescence studies, cells grown on coverslips were washed in PBS, fixed in a solution containing 3.7% paraformaldehyde and 30 mM sucrose, for 30 min at 4°C. The cells were washed once in PBS, and after quenching for 10 min in PBS containing 50 mM NH4Cl, washed again in PBS supplemented with 1 mg/ml BSA. The cells were incubated with primary antibodies in permeabilization buffer A (PBS containing 1 mg/ml BSA and 0.05% saponin) for 45 min at room temperature. After two washes in the same buffer A, the cells were incubated for 45 min at room temperature in buffer A containing the labeled secondary antibody. After two washes in buffer A and one in PBS, the cells were mounted on microscope slides in 100 mM Tris-HCl buffer (pH 8.5) containing 100 mg/ml Mowiol (Calbiochem) and 25% glycerol (v/v).

The samples were examined under an epifluorescence microscope (Axioplan II, Zeiss) attached to a cooled CCD-camera (Spot-2, Diagnostic Instruments) or under a confocal microscope (LSM 510, Zeiss).

Antibodies used were: monoclonal mouse antibodies 100.3 against  $\gamma$ -adaptin and 100.1 against  $\beta$ -adaptins (Sigma, [14]); affinity-purified rabbit polyclonal anti-Eps15 antibody [46]; Alexa 488 goat anti-mouse immunoglobulins; and Alexa 594-conjugated goat anti-rabbit immunoglobulins (Molecular Probes).

##### Acknowledgments

We should like to thank Adriana Miele for assistance with A753D structure, Yann Goureau for expert assistance in confocal microscopy, and Airlie McCoy and Margaret Robinson for reading the manuscript. D.J.O. is funded by a Wellcome Trust Senior Research Fellow in Basic Biomedical Science, and A.B. is funded by the Association pour la Recherche contre le Cancer (ARC, grant number 5807).

Received: February 21, 2002

Revised: May 9, 2002

Accepted: May 13, 2002

##### References

1. Puertollano, R., Randazzo, P.A., Presley, J.F., Hartnell, L.M., and Bonifacino, J.S. (2001). The GGAs promote ARF-dependent recruitment of clathrin to the TGN. *Cell* 105, 93–102.
2. Puertollano, R., Aguilar, R.C., Gorshkova, I., Crouch, R.J., and Bonifacino, J.S. (2001). Sorting of mannose 6-phosphate receptors mediated by the GGAs. *Science* 292, 1712–1716.
3. Nielsen, M.S., Madsen, P., Christensen, E., Nykjaer, A., Glieemann, J., Kaspar-Biermann, D., Pohlmann, R., and Petersen, C.M. (2001). The sortilin cytoplasmic tail conveys Golgi-endo-

some transport and binds the VHS domain of the GGA2 sorting protein. *EMBO J.* 20, 2180–2190.

- 4. Zhu, Y.X., Doray, B., Poussu, A., Lehto, V.P., and Kornfeld, S. (2001). Binding of GGA2 to the lysosomal enzyme sorting motif of the mannose 6-phosphate receptor. *Science* 292, 1716–1718.
- 5. Itoh, T., Koshiba, S., Kigawa, T., Kikuchi, A., Yokoyama, S., and Takenawa, T. (2001). Role of the ENTH domain in phosphatidyl-inositol-4,5-bisphosphate binding and endocytosis. *Science* 291, 1047–1051.
- 6. Ford, M.G., Pearse, B.M., Higgins, M.K., Vallis, Y., Owen, D.J., Gibson, A., Hopkins, C.R., Evans, P.R., and McMahon, H.T. (2001). Simultaneous binding of PtdIns(4,5)P<sub>2</sub> and clathrin by AP180 in the nucleation of clathrin lattices on membranes. *Science* 291, 1051–1055.
- 7. Shih, W., Gallusser, A., and Kirchhausen, T. (1995). A clathrin-binding site in the hinge of the beta 2 chain of mammalian AP-2 complexes. *J. Biol. Chem.* 270, 31083–31090.
- 8. Yeung, B.G., and Payne, G.S. (2001). Clathrin interactions with C-terminal regions of the yeast AP-1 beta and gamma subunits are important for AP-1 association with clathrin coats. *Traffic* 2, 565–576.
- 9. Ohno, H., Stewart, J., Fournier, M.C., Bosshart, H., Rhee, I., Miyatake, S., Saito, T., Gallusser, A., Kirchhausen, T., and Bonifacino, J.S. (1995). Interaction of tyrosine-based sorting signals with clathrin-associated proteins. *Science* 269, 1872–1875.
- 10. Gaidarov, I., Chen, Q., Falck, J.R., Reddy, K.K., and Keen, J.H. (1996). A functional phosphatidylinositol 3,4,5-trisphosphate/phosphoinositide binding domain in the clathrin adaptor Ap-2 alpha subunit—implications for the endocytic pathway. *J. Biol. Chem.* 271, 20922–20929.
- 11. Kirchhausen, T. (1999). Adaptors for clathrin-mediated traffic. *Annu. Rev. Cell Dev. Biol.* 15, 705–732.
- 12. Robinson, M.S., and Bonifacino, J.S. (2001). Adaptor-related proteins. *Curr. Opin. Cell Biol.* 13, 444–453.
- 13. Robinson, M.S. (1990). Cloning and expression of gamma-adaptin, a component of clathrin-coated vesicles associated with the Golgi apparatus. *J. Cell Biol.* 111, 2319–2326.
- 14. Ahle, S., Mann, A., Eichelsbacher, U., and Ungewickell, E. (1988). Structural relationships between clathrin assembly proteins from the Golgi and the plasma membrane. *EMBO J.* 7, 919–929.
- 15. Futter, C., Gibson, A., Allchin, E., Maxwell, S., Ruddock, L., Odorizzi, G., Domingo, D., Trowbridge, I., and Hopkins, C. (1998). In polarized MDCK cells basolateral vesicles arise from clathrin-gamma-adaptin-coated domains on endosomal tubules. *J. Cell Biol.* 141, 611–623.
- 16. Robinson, M.S. (1987). 100-kD coated vesicle proteins: molecular heterogeneity and intracellular distribution studied with monoclonal antibodies. *J. Cell Biol.* 104, 887–895.
- 17. Owen, D.J., and Evans, P.R. (1998). A structural explanation for the recognition of tyrosine-based endocytotic signals. *Science* 282, 1327–1332.
- 18. Rapoport, I., Chen, Y.C., Cupers, P., Shoelson, S.E., and Kirchhausen, T. (1998). Dileucine-based sorting signals bind to the beta chain of AP-1 at a site distinct and regulated differently from the tyrosine-based motif-binding site. *EMBO J.* 17, 2148–2155.
- 19. Rodionov, D.G., and Bakke, O. (1998). Medium chains of adaptor complexes ap-1 and ap-2 recognize leucine-based sorting signals from the invariant chain. *J. Biol. Chem.* 273, 6005–6008.
- 20. ter Haar, E., Harrison, S.C., and Kirchhausen, T. (2000). Peptide-in-groove interactions link target proteins to the beta-propeller of clathrin. *Proc. Natl. Acad. Sci. USA* 97, 1096–1100.
- 21. Dell'Angelica, E.C., Klumperman, J., Stoorvogel, W., and Bonifacino, J.S. (1998). Association of the AP-3 adaptor complex with clathrin. *Science* 280, 431–434.
- 22. Doray, B., and Kornfeld, S. (2001). Gamma subunit of the AP-1 adaptor complex binds clathrin: Implications for cooperative binding in coated vesicle. *Mol. Biol. Cell* 12, 1925–1935.
- 23. Benmerah, A., Bègue, B., Dautry-Varsat, A., and Cerf-Bensussan, N. (1996). The ear of alpha-adaptin interacts with the COOH-terminal domain of the Eps15 protein. *J. Biol. Chem.* 271, 12111–12116.
- 24. Chen, H., Fre, S., Slepnev, V.I., Capua, M.R., Takei, K., Butler, M.H., Di Fiore, P.P., and De Camilli, P. (1998). Epsin is an EH-domain-binding protein implicated in clathrin-mediated endocytosis. *Nature* 394, 793–797.
- 25. Owen, D.J., Vallis, Y., Noble, M.E., Hunter, J.B., Dafforn, T.R., Evans, P.R., and McMahon, H.T. (1999). A structural explanation for the binding of multiple ligands by the alpha-adaptin appendage domain. *Cell* 97, 805–815.
- 26. Owen, D.J., Vallis, Y., Pearse, B.M., McMahon, H.T., and Evans, P.R. (2000). The structure and function of the beta2-adaptin appendage domain. *EMBO J.* 19, 4216–4227.
- 27. David, C., McPherson, P.S., Munndig, O., and De Camilli, P. (1996). A role of amphiphysin in synaptic vesicle endocytosis suggested by its binding to dynamin in nerve terminals. *Proc. Natl. Acad. Sci. USA* 93, 331–335.
- 28. Traub, L.M., Downs, M.A., Westrich, J.L., and Fremont, D.H. (1999). Crystal structure of the alpha appendage of AP-2 reveals a recruitment platform for clathrin-coat assembly. *Proc. Natl. Acad. Sci. USA* 96, 8907–8912.
- 29. Page, L.J., Sowerby, P.J., Lui, W.W., and Robinson, M.S. (1999). Gamma-synergin: an EH domain-containing protein that interacts with gamma-adaptin. *J. Cell Biol.* 146, 993–1004.
- 30. Takatsu, H., Yoshino, K., and Nakayama, K. (2000). Adaptor gamma ear homology domain conserved in gamma-adaptin and GGA proteins that interact with gamma-synergin. *Biochem. Biophys. Res. Commun.* 271, 719–725.
- 31. Hirst, J., Lui, W.W., Bright, N.A., Totty, N., Seaman, M.N., and Robinson, M.S. (2000). A family of proteins with gamma-adaptin and VHS domains that facilitate trafficking between the trans-Golgi network and the vacuole/lysosome. *J. Cell Biol.* 149, 67–80.
- 32. Dell'Angelica, E.C., Puertollano, R., Mullins, C., Aguilar, R.C., Vargas, J.D., Hartnell, L.M. and Bonifacino, J.S. (2000). GGA's: a family of ADP ribosylation factor-binding proteins related to adaptors and associated with the Golgi complex. *J. Cell Biol.* 149, 81–93.
- 33. Tebar, F., Sorkina, T., Sorkin, A., and Kirchhausen, T. (1996). Eps15 is a component of clathrin-coated pits and vesicles and is located at the rim of coated pits. *J. Biol. Chem.* 271, 28727–28730.
- 34. Torrisi, M.R., Lotti, L.V., Belleudi, F., Gradi, R., Salcini, A.E., Confalonieri, S., Pelicci, P.G., and Di Fiore, P.P. (1999). Eps15 is recruited to the plasma membrane upon epidermal growth factor receptor activation and localizes to components of the endocytic pathway during receptor internalization. *Mol. Biol. Cell* 10, 417–434.
- 35. Robinson, M.S., and Kreis, T.E. (1992). Recruitment of coat proteins onto Golgi membranes in intact and permeabilized cells: effects of brefeldin A and G protein activators. *Cell* 69, 129–138.
- 36. de Beer, T., Carter, R.E., Lobel-Rice, K.E., Sorkin, A., and Overduin, M. (1998). Structure and Asn-Pro-Phe binding pocket of the Eps15 homology domain. *Science* 281, 1357–1360.
- 37. Boehm, M., and Bonifacino, J.S. (2001). Adaptins: the final recount. *Mol. Biol. Cell* 12, 2907–2920.
- 38. Stammes, M.A., and Rothman, J.E. (1993). The binding of AP-1 clathrin adaptor particles to Golgi membranes requires ADP-ribosylation factor, a small GTP-binding protein. *Cell* 73, 999–1005.
- 39. Santolini, E., Salcini, A.E., Kay, B.K., Yamabhai, M., and Di Fiore, P.P. (1999). The EH network. *Exp. Cell Res.* 253, 186–209.
- 40. Leslie, A.G.W. (1992). Recent changes to the MOSFLM package for processing film and image plate data. In *Joint CCP4 and ESF-EACMB Newsletter on Protein Crystallography*, No. 26 (Warrington, UK: Daresbury Laboratory).
- 41. CCP4 (Collaborative Computational Project 4) (1994). The CCP4 suite: programs for protein crystallography. *Acta Crystallogr. D* 50, 760–763.
- 42. de la Fortelle, E., and Bricogne, G. (1997). Maximum-likelihood heavy-atom parameter refinement for multiple isomorphous replacement and multiwavelength anomalous diffraction methods. In *Methods in Enzymology*, Volume 276, C.W. Carter, Jr., and R.M. Sweet, eds. (New York: Academic Press), pp. 472–494.
- 43. Abrahams, J.P., and Leslie, A.G.W. (1996). Methods used in the structure determination of bovine mitochondrial F1 ATPase. *Acta Crystallogr. D* 52, 30–42.

44. Jones, T.A., Zou, J.Y., Cowan, S.W. and Kjeldgaard, M. (1991). Improved methods for building protein models in electron density maps and the location of errors in these models. *Acta Crystallogr. A* 47, 110–119.
45. Murshudov, G.N., Vagin, A.A., and Dodson, E.J. (1997). Refinement of macromolecular structures by the maximum-likelihood method. *Acta Crystallogr. D* 53, 240–255.
46. Scott, M.G., Benmerah, A., Muntaner, O., and Marullo, S. (2001). Recruitment of activated G protein-coupled receptors to pre-existing clathrin-coated pits in living cells. *J. Biol. Chem.* 277, 3552–3559.

**Accession Numbers**

The coordinates and structure factors have been deposited in the Protein Data Bank, accession codes 1GYU (wild-type), 1GYV (L662E mutant), and 1GYW (A753D mutant).